Probe sonication-assisted rapid synthesis of highly fluorescent sulfur quantum dots

Kadian, Sachin; Chaulagain, Narendra; Joshi, Naveen Narasimhachar; Alam, Kazi Mohammad; Cui, Kai; Shankar, Karthik; Manik, Gaurav; Narayan, Roger

Publisher's version / Version de l'éditeur:
https://doi.org/10.1088/1361-6528/acd00a
Nanotechnology, 34, 30, 2023-05-09

Nanotechnology

Probe sonication-assisted rapid synthesis of highly fluorescent sulfur quantum dots

To cite this article before publication: Sachin Kadian *et al* 2023 *Nanotechnology* in press https://doi.org/10.1088/1361-6528/acd00a

Probe sonication-assisted rapid synthesis of highly fluorescent sulfur quantum dots

Sachin Kadian[1,2,5], Narendra Chaulagain[2], Naveen Narasimhachar Joshi[3], Kazi M. Alam[2], Kai Cui[4], Karthik Shankar[2, *], Gaurav Manik[1, *] and Roger J Narayan[3,5, *]

[1]*Department of Polymer and Process Engineering, Indian Institute of Technology Roorkee, Uttarakhand, India-247667*

[2]*Department of Electrical and Computer Engineering, University of Alberta, Edmonton, AB T6G 1H9, Canada*

[3]*Department of Materials Science and Engineering, Centennial Campus North Carolina State University, Raleigh, North Carolina 27695-7907, USA*

[4]*Nanotechnology Research Centre, National Research Council Canada, Edmonton, AB T6G 2M9, Canada*

[5]*Joint Department of Biomedical Engineering, University of North Carolina and North Carolina State University, Raleigh, NC 27695, USA*

**Corresponding authors*

Probe sonication-assisted rapid synthesis of highly fluorescent sulfur quantum dots

Abstract

A new type of heavy-metal free single-element nanomaterial, called sulfur quantum dots (SQDs), has gained significant attention due to its advantages over traditional semiconductor QDs for several biomedical and optoelectronic applications. A straightforward and rapid synthesis approach for preparing highly fluorescent SQDs is needed to utilize this nanomaterial for technological applications. Until now, only a few synthesis approaches have been reported; however, these approaches are associated with long reaction times and low quantum yields (QY). Herein, we propose a novel optimized strategy to synthesize SQDs using a mix of probe sonication and heating, which reduces the reaction time usually needed from 125 h to a mere 15 min. The investigation employs cavitation and vibration effects of high-energy acoustic waves to break down the bulk sulfur into nano-sized particles in the presence of highly alkaline medium and oleic acid. In contrast to previous reports, the obtained SQDs exhibited excellent aqueous solubility, desirable photostability, and a relatively high photoluminescence QY up to 10.4% without the need of any post-treatment. Additionally, the as-synthesized SQDs show excitation-dependent emission and excellent stability in different pH (2−12) and temperature (20-80 °C) environments. Hence, this strategy opens a new pathway for rapid synthesis of SQDs and may facilitate the use of these materials for biomedical and optoelectronic applications.

Keywords: sulfur quantum dots, probe sonication, fluorescent nanomaterials, photostability, and quantum yield

1. Introduction

Colloidal quantum dots (QDs), which exhibit size-dependent optical, biological, chemical and electronic properties, have recently captured significant attention from academia and industry because of their wide potential for use in biomedical and optoelectronic devices [1][2][3][4][5][6]. However, conventional semiconductor QDs (e.g., CdS, CdSe, PbS, and CdTe) are limited in their potential commercial use due to their composition, particularly the presence of toxic heavy metals [7][8][9][10]. Similarly, all-inorganic perovskite QDs $CsPbX_3$ (X = Br, I, Cl) have been considered for optoelectronics applications due to their favorable optical and electronics features [11–14]. Over the last decade, researchers have considered approaches to create non-toxic QDs from elements such as carbon [15][16][17], silicon [18][19], phosphorus [20][21] and sulfur (S) [22]. Owing to their excellent photostability, aqueous solubility, and low toxicity, these heavy metal-free QDs are considered to be promising next generation fluorescent nanomaterials [23,24]. Although elemental S offers several unique merits such as involuntary production, natural abundance, and inherent antibacterial characteristics [25][26][27], sulfur QDs (SQDs) have rarely been explored due to the challenges associated with producing highly fluorescent SQDs via a straightforward approach. For example, in 2014, Li et al. prepared luminescent S-dots by etching the Cd part of CdS QDs through a phase interfacial reaction but achieved a relatively low photoluminescent (PL) quantum yield (QY) of 0.549% [22]. In 2018, Shen et al. proposed an "assemble-fission" strategy involving the exposure of sublimated sulfur powder to alkali and the use of polyethylene glycol-400 as a passivation agent; they synthesized polyethylene glycol (PEG) functionalized SQDs with an increased QY up to 3.8% [28]. Later, Wang et al. showed that the QY of SQDs prepared via this method could be significantly enhanced to up to 23% through hydrogen peroxide treatment [29]. Nevertheless, the above-discussed methods need more than 125 h of time to complete the reaction steps [22][29]. Recently, Sun and colleagues reduced the reaction time to 4 h and prepared fluorescent S-dots with a QY up to 4.02% using bulk S, sodium hydroxide (NaOH), and PEG as precursors through a straightforward hydrothermal process [30]. At this time, a limited number of synthesis strategies have been reported for the preparation of SQDs; hence, a straightforward and rapid approach to create SQDs with a high QY is highly desirable [31]. Herein, we report a novel, straightforward, and rapid strategy to synthesize highly fluorescent SQDs in 15 min. In this approach, the cavitation and vibration effects of an ultrasonic probe sonicator were used to break down the bulk S into nano-sized particles in the alkaline environment, followed by heating as illustrated in Scheme 1. The SQDs synthesized through this probe sonication-assisted strategy were evaluated using several characterization techniques, including photoluminescence (PL), UV-visible absorption, Fourier transform infrared

spectroscopy (FTIR), X-ray photoelectron spectroscopy (XPS), X-ray diffraction (XRD), Raman spectroscopy, and transmission electron microscopy (TEM). The as-prepared blue fluorescent SQDs demonstrated excellent photostability and aqueous solubility, with a QY up to 10.4%. To the best of our knowledge, this is the first report of the rapid synthesis of highly fluorescent water-soluble SQDs.

2. Experimental section

2.1 Materials and chemicals

Bulk sulfur (S), a fine yellow color powder with 98% purity and 32.06 g/mol molecular weight, was purchased from Sisco Research Laboratories Pvt. Ltd. (Mumbai, Maharashtra, India). NaOH pellets and oleic acid were obtained from Merck Ltd (Mumbai, Maharashtra, India). All chemicals were of analytical grade and used without any further purification. For all experiments, dilutions, solutions and washing, fresh Millipore system-purified water was used.

2.2 Synthesis of SQDs

The SQDs were synthesized using a straightforward top-down approach that used the cavitation and vibration effects of ultrasonic waves. In this approach, 0.3 g bulk S, 2.0 g NaOH, 0.5 mL oleic acid and 20 mL water were mixed in a small beaker as shown in Scheme 1. The mixture was allowed to react for 3 min under high amplitude ultrasonic waves using a probe sonication instrument (500-watt, 20 kHz) with a pulse on and off time of 5 s. The obtained frothy mixture was allowed to condense via a heating process by exposure to a hot plate at 190 °C for 8, 10, 12, and 14 min. The resultant pale-yellow color aqueous solution (containing SQDs) in the lower part of beaker was filtered through a syringe filter followed by centrifuging and dialysis using 1kDa molecular weight-cutoff membrane. To understand the effect of probe sonication assistance, a mixture of all of the precursors was directly subjected to heat for the same duration under similar experimental conditions and filtered in a similar manner. The purified samples with and without probe sonication were stored in a refrigerator until further characterization was performed.

2.3 Physical and chemical characterization

A Cary 5000 UV-Vis-NIR spectrometer (Agilent, Santa Clara, CA) and a Hitachi F-4600 fluorescence spectrophotometer (Hitachi, Tokyo, Japan) were used to obtain the UV-Vis absorption and PL spectra of the as-synthesized SQDs, respectively. FTIR spectra were recorded using a C91158 spectrometer (PerkinElmer, Waltham, MA). A D8-Advance X-ray

diffractometer (Bruker Corporation, Billerica, MA) operating at a scan rate of 4°/min was used to obtain the XRD patterns of the as-prepared SQDs. A PHI 5000 VersaProbe III instrument (Physical Electronics, Inc., Chanhassen, MN) was used to collect the XPS spectra of the as-synthesized SQDs. TEM imaging for evaluating the morphology and particle size of SQDs were obtained using a Tecnai G^2 20 S-TWIN instrument (FEI Company, Hillsboro, OR). High resolution TEM images were captured using H9500 TEM instrument (Hitachi, Tokyo, Japan), which was equipped with a LaB_6 emission gun. Electron energy-loss spectroscopy (EELS) under the TEM imaging mode was used to obtain the inner-shell ionization edge (core loss) spectra; a GIF Tridium spectrometer (Gatan Inc. Pleasanton, CA) was used to obtain the EELS data. A inVia Qontor confocal Raman microscope (Renishaw plc, Wotton-under-Edge, United Kingdom) was used to collect the Raman spectra of the as-synthesized SQDs. The ultrasonication treatment was performed using a Sonics Vibra-Cell™ Model CV334 probe sonication instrument (Sonics & Materials, Inc., Newtown, CT).

2.4 Quantum yield measurement of SQDs

The QY of as-prepared SQDs was estimated using an approach that was reported previously[22]·[32]. In this approach, quinine sulfate was taken as a reference with known QY of 0.54; the following equation was used to calculate the QY of SQDs:

$$Q = \mathrm{Q_R} \times \left(\frac{I}{I_R}\right) \times \left(\frac{A_R}{A}\right) \times \left(\frac{\eta}{\eta_R}\right)^2 \quad \ldots(1)$$

where Q_R, I_R, A_R, and η_R represent QY, measured integrated emission intensity (area under the curve between 375-700 nm), absorbance at 360 nm, and refractive index of the known reference, respectively. In the equation, Q, I, A and η denote QY, measured integrated emission intensity (area under the curve between 375-700 nm), absorbance at 360 nm, and refractive index of SQDs, respectively.

3. Results and discussion

In this study, we have synthesized SQDs by breaking down bulk S into nano-sized particles through the cavitation and vibration effects of high energy acoustic waves (Scheme 1). Initially, 0.3 g bulk S is mixed into 20 mL aqueous NaOH solution in the presence of oleic acid. The mixture is subjected to react for 3 min under high amplitude ultrasonic waves using a probe sonication instrument (500-watt, 20 kHz) with a pulse on and off time of 5 s. Previous reports indicate that strong expansive and compressive acoustic waves generate cavities (bubbles) in the liquid and make them oscillate [33].

Under appropriate conditions, these bubbles overgrow and later collapse, releasing the high energy stored inside the cavities within a very short span of time [33]. This implosive collapse of cavities is localized and momentary; however, it generates high pressure waves and temperatures that support the breakdown of bulk S into nano-sized particles. The double bond of existing oleic acid undergoes an oxidative cleavage [34,35] that results in the formation of nonanoic acid and azelaic acid [34]. These products prevent the reassembling process of as-generated nanoparticles through their effective surface passivation, resulting in the production of a frothy mixture. The obtained frothy mixture is allowed to condense through a heating process that involves exposure to a hot plate at 190 °C. The resultant transparent pale-yellow color aqueous solution in the lower part of the beaker indicates the formation of SQDs.

In order to optimize the synthesis process, the time duration of heating process was varied from 8 to 14 min with a time interval of 2 min. To understand the impact of probe sonication step, the entire experiment was repeated without ultrasonication treatment of precursor mixture; the resultant control sample was used for comparison purposes. Fig. 1a and inset show the UV-Vis absorption and PL spectra of SQDs and non-fluorescent S-dots prepared with and without probe sonication assistance, respectively. The UV-visible spectra of non-fluorescent S-dots show two absorption bands at 304 nm and 370 nm; these features are ascribed to the presence of S_2^{2-} and S_3^{2-} adsorbed on the surface of S-dots (similar to previous reports) [28][29][36]. After the probe sonication treatment, a blue-shift in peak from 304 to 295 nm and a decrease in the intensity of band at 370 nm was observed; these features can be assigned to etching or breakdown of surface S_x^{2-} species and quantum size confinement of SQDs [29]. To further validate the UV-visible results, the PL spectra of both samples were acquired; these spectra are shown in the inset of Fig. 1a. It can be observed that the probe sonication-treated SQDs exhibit a strong PL emission intensity band at 465 nm; the PL emission spectra of untreated non-fluorescent S-dots was comparatively flat. These results confirm that the probe sonication step plays a key role in the synthesis of highly fluorescent SQDs. Further, to optimize the effect of heating time on the fluorescence of SQDs, the PL spectra of all of the samples (8, 10, 12, and 14 min) were collected; these results are shown in Fig. 1b. Fig. 1b shows that as the heating time was increased up to 12 min, the fluorescence intensity of SQDs continued to increase. Beyond 12 min, an apparent sharp decrease in the fluorescence intensity was observed (i.e., when heating was extended to 14 min). This decrease in fluorescence intensity can be ascribed to re-aggregation of monodispersed SQDs; these findings are similar to earlier reports by Sun and co-workers [30].

To better understand the abovementioned optical spectroscopy results, morphological characterization of non-fluorescent S-dots obtained after 14 min heating without any probe sonication treatment and fluorescent SQDs prepared with probe sonication followed by 12 min and 14 min heating were performed using TEM; these results are shown in Fig. 2. The TEM micrograph (Fig. 2a) of non-fluorescent S-dots indicates the formation of a non-uniform assembly of relatively large size nanoparticles with particle size varying between 30 nm to 80 nm (average size ~55 nm) (Fig. 2b). The TEM image (Fig. 2c and 2g) of SQDs synthesized through probe sonication followed by 12 min heating exhibit excellent uniformity and dispersibility in an aqueous medium, with an average particle size of ~10 nm (Fig. 2d and 2g). Interestingly, the TEM image (Fig. 2e) of SQDs obtained using probe sonication followed by 14 min heating process shows the aggregation of mono-dispersed particles as indicated by the yellow color arrow; an increase in the range of the size distribution histogram (Fig. 2f) from ~10 nm to ~22 nm and an average particle size diameter of ~22 nm were noted. These TEM results appear to corroborate our hypothesis that increasing the heating time beyond 12 min encourages the surface interaction of different particles and leads to their aggregation; this finding is consistent with the optical spectroscopy results. The phenomenon of aggregation due to overheating was also previously observed by Sun and co-workers [30]. Therefore, these results enable us to conclude that highly fluorescent SQDs can be synthesized quickly in a total of 15 min of time (3 min sonication followed by 12 min of heating) at 190 °C. Next, the optimized SQDs were characterized through a series of advanced characterization techniques to confirm their successful synthesis. The high-resolution TEM image (Fig. 2g) depicts the ordered and parallel lattice fringes of SQDs with a spacing of 0.21 nm, which corresponds to the orthorhombic (S_8) phase of S [37,38].

To understand the optical features of the SQDs, PL emission spectra were recorded at different excitation wavelengths ranging from 300 to 400 nm (Fig. 3a). The PL emission spectra indicated that the SQDs exhibit an excitation-dependent emission, with a red-shift in the emission peak from 420 to 480 nm and a maximum emission peak at 465 nm when excited at 360 nm wavelength. These results are consistent with previous findings by Wu and colleagues [22]. This excitation-dependent emission behavior can be ascribed to the inherent complexity of the excited states of SQDs [22]. Next, the fluorescence QY of as-prepared SQDs in water was calculated through a well-established reference method [32] and was estimated to be 10.4% relative to quinine sulfate in 1mM aqueous H_2SO_4; this result is better than some of those described in previous reports and comparable to others as listed in Table 1. Further, the photostability of as-synthesized SQDs was investigated under continuous exposure to 360 nm wavelength UV radiation from a 150 W Xenon lamp for 20

min (Fig. 3b). It was observed that approximately 98% of the initial PL intensity is still preserved, which attests to the excellent photostability of the material.

Furthermore, the stability of SQDs in different pH environments and temperatures is important to understand their potential use for biomedical applications. Hence, the effect of pH on the PL intensity of SQDs was explored in different pH environments (ranging from 2 to 12) and temperatures (20-80 °C); the results are shown in the inset of Fig. 3b. It was shown that the PL intensity of as-prepared SQDs increased with increasing pH from 2 to 7 and was almost constant between pH values of 7 to 12. Furthermore, the PL intensity of the SQDs was found to be stable until 40 °C, a slight decrease in the PL intensity was observed as the temperature was increased up to 80 °C. This result may be due to the surface interaction of different particles. These results suggest that the as-synthesized SQDs possess excellent photostability and high fluorescence under many pH and temperature conditions with a favorable QY. The XRD pattern (Fig. 3c) of the SQDs revealed the existence of both the hexagonal (S_6) and orthorhombic (S_8) phase, which is in good agreement with TEM results shown in (Fig. 2g) and earlier reports by Xiao et al. [30].

To better understand the synthesized SQDs, EELS and Raman spectra of the as-prepared SQDs were recorded and are shown in Fig. 4. The results shown in Fig. 4a indicate that the EELS spectrum exhibits three prominent peaks at 165 eV, 283 eV and 534 eV. The broad peak starting at 165 eV corresponds to S-$L_{2,3}$ edge of SQDs, whereas the peak starting at 283 eV and 534 eV are assigned to C-K edge and O-K edge, respectively; these results are in accordance with those in the literature [39,40]. Furthermore, the Raman spectra (Fig. 4b) of SQDs demonstrate five main peaks centered at Raman shifts of 150, 218, 246, 440 and 472 cm^{-1}; these results are in good agreement with previous reports and suggest the formation of SQDs [41,42].The presence of these characteristic peaks in the XRD, EELS and Raman spectra enable us to conclude that the water-soluble SQDs have been successfully synthesized.

Next, to gain an insight into the interaction between oleic acid and S, FTIR spectra of SQDs and pure oleic acid were recorded; the results are shown in Fig. 4c. The broad peak centered at 3280 cm^{-1} in both curves is ascribed to the O-H stretching of carboxylic groups in oleic acid and adsorbed water [43]. The peaks at 2898 cm^{-1} can be assigned to symmetric stretching of -CH_2 present in the chain of oleic acid [44]. Further, the bands at 1715 cm^{-1} and 1630 cm^{-1} are attributed to carboxylic moieties through asymmetric and symmetric C=O stretching, respectively. The two peaks located at 1464 cm^{-1} and [illegible] cm^{-1} denote the in-plane and out-of-plane stretching of the O-H bond, respectively [44][45]. In contrast, the FTIR

spectra of SQDs exhibit a shift in peak location from 2898 cm^{-1} to 2882 cm^{-1}, corresponding to symmetric stretching of -CH_2; the merging of bands at 1715 cm^{-1} and 1630 cm^{-1} into a single peak at 1650 cm^{-1} corresponds to asymmetric and symmetric C=O stretching. Further, the peaks corresponding to in-plane (1464 cm^{-1}) and out-of-plane (997 cm^{-1}) O-H stretching were noted to be shifted to wavenumbers 1398 cm^{-1} and 978 cm^{-1}, respectively. The shift towards lower wavenumbers (from 1464 cm^{-1} to 1398 cm^{-1} and from 997 cm^{-1} to 978 cm^{-1}) is attributed to the cleavage of the double bond present in the alkyl chain of oleic acid during oxidation and the formation into hydrophilic carboxyl groups on the surface of SQDs. Another peak located at 1105 cm^{-1} in SQDs can be ascribed to the occurrence of S-related groups (e.g., sulfide and sulfone) [46][47]. Therefore, the occurrence of relevant peaks in the FTIR spectra of SQDs and pure oleic acid illustrates that oleic acid molecules have primarily helped in the synthesis of SQDs by preventing their reaggregation and providing water solubility through existing hydrophilic carboxyl groups on the surface.

Additionally, X-ray photoelectron spectroscopy analysis was performed to examine the elemental and chemical composition of SQDs (as shown in Fig. 5). The XPS spectrum (Fig. 5a) shows that the formation of SQDs primarily involves C, O, and S. Next, to gain more insight about the structure of the SQDs, the high-resolution deconvoluted spectra of S 2*p* was also analyzed (as shown in Fig. 5b). The deconvoluted S 2*p* spectrum consists of six peaks at binding energies 160.8 eV, 161.9 eV, 163.05 eV, 165.5 eV, 166.5 eV and 167.7 eV. The bands located at binding energies 160.8 eV, 161.9 eV and 163.05 eV are ascribed to atomic S; those at 165.5 eV, 166.5 eV, and 167.7 eV are attributed to oxidized forms (e.g., SO_x^- and SO_x^{2-}) of S[48,49]. Consequently, it can be inferred that SQDs mainly consist of atomic S, sulfonate, sulfite, and sulfonyl groups; these findings are consistent with those of previous reports[28][30][50]. Based on these results, it can be concluded the probe sonication approach is associated with the synthesis of highly fluorescent water-soluble SQDs.

Furthermore, a comparison between our proposed strategy and previously reported approaches for the synthesis of SQDs is listed in Table 1. The comparison table suggests that our proposed strategy is superior to all previously reported methods in terms of reaction time; in addition, it appears to be comparable with best-performing approaches in terms of QY. These results indicate that our proposed approach is associated with a remarkable reduction in reaction time and favorably high QY.

4. Conclusions and future recommendations

In this study, we have employed a novel route for the rapid synthesis of highly fluorescent SQDs that uses the assistance of probe sonication. The as-synthesized SQDs demonstrated excellent optical and generally desirable properties, including aqueous solubility, photostability, and relatively high fluorescence QY up to 10.4% with a maximum emission at 465 nm; these properties were obtained without the need of any post-treatment. The cavitation and vibration effects involved with probe sonication accounted for the breakdown of bulk S into nano-sized particles. In addition, the as-prepared SQDs exhibited excitation-dependent emission behavior, which was attributed to the complexity of excited states. Moreover, the as-prepared SQDs demonstrated excellent stability in different pH (2–12) and temperature (20-80 °C) environments with sustained PL intensity. Furthermore, based on optical spectroscopic and TEM results, we propose a process involving 3 min probe sonication followed by 12 min heat for the synthesis of SQDs with optimal properties. Since post-treatment approaches may improve the characteristics of various types of QDs, it can be anticipated that the fluorescence QY of SQDs prepared via our proposed strategy could be enhanced by an appropriate post-treatment such as H_2O_2-assisted etching of polysulfide groups. Our group is still working to further enhance the optical properties of SQDs; this investigation shall be part of a future submission. The exciting results that were obtained from untreated SQDs synthesized via probe sonication assistance suggest that SQDs possess significant potential for biomedical and optoelectronic applications.

Conflicts of interests

There are no conflicts to declare for this study.

Acknowledgments

S.K. would like to thank the Science and Engineering Research Board (SERB), Department of Science and Technology, Government of India for facilitating with overseas visiting doctoral fellowship (OVDF). The authors would like to acknowledge direct and indirect support from the Future Energy Systems (FES) at the University of Alberta and the National Research Council Canada (NRC). The authors sincerely thank the Department of Polymer and Process Engineering, IIT Roorkee, and the Department of Electrical & Computer Engineering, the University of Alberta, for providing the infrastructure to complete this study.

References

[1] Colvin V L, Schlamp M C and Alivisatos A P 1994 Light-emitting diodes made from cadmium selenide nanocrystals and a semiconducting polymer *Nature* **370**

[2] Fan F, Voznyy O, Sabatini R P, Bicanic K T, Adachi M M, McBride J R, Reid K R, Park Y S, Li X, Jain A, Quintero-Bermudez R, Saravanapavanantham M, Liu M, Korkusinski M, Hawrylak P, Klimov V I, Rosenthal S J, Hoogland S and Sargent E H 2017 Continuous-wave lasing in colloidal quantum dot solids enabled by facet-selective epitaxy *Nature* **544**

[3] Kadian S, Sethi S K and Manik G 2021 Recent advancements in synthesis and property control of graphene quantum dots for biomedical and optoelectronic applications *Mater Chem Front* **5**

[4] Chatterjee M, Nath P, Kadian S, Kumar A, Kumar V, Roy P, Manik G and Satapathi S 2022 Highly sensitive and selective detection of dopamine with boron and sulfur co-doped graphene quantum dots *Sci Rep* **12**

[5] Kumar R, Kumar J, Kadian S, Srivastava P, Manik G and Bag M 2021 Tunable ionic conductivity and photoluminescence in quasi-2D CH3NH3PbBr3 thin films incorporating sulphur doped graphene quantum dots *Phys. Chem. Chem. Phys.* **23** 22733–42

[6] Chaulagain N, Alam K M, Kadian S, Kumar N, Garcia J, Manik G and Shankar K 2022 Synergistic Enhancement of the Photoelectrochemical Performance of TiO2 Nanorod Arrays through Embedded Plasmon and Surface Carbon Nitride Co-sensitization *ACS Appl Mater Interfaces* **14** 24309–20

[7] Kumari P and Toshniwal D 2019 Hourly solar irradiance prediction from satellite data using lstm

[8] Chen B, Pradhan N and Zhong H 2018 From Large-Scale Synthesis to Lighting Device Applications of Ternary I-III-VI Semiconductor Nanocrystals: Inspiring Greener Materials Emitters *Journal of Physical Chemistry Letters*

[9] Zhang F, Zhong H, Chen C, Wu X G, Hu X, Huang H, Han J, Zou B and Dong Y 2015 Brightly luminescent and color-tunable colloidal CH3NH3PbX3 (X = Br, I, Cl) quantum dots: Potential alternatives for display technology *ACS Nano*

[10] Xu G, Zeng S, Zhang B, Swihart M T, Yong K T and Prasad P N 2016 New Generation Cadmium-Free Quantum Dots for Biophotonics and Nanomedicine *Chem Rev*

[11] Li X, Ma W, Liang D, Cai W, Zhao S and Zang Z 2022 High-performance CsPbBr3@Cs4PbBr6/SiO2 nanocrystals via double coating layers for white light emission and visible light communication *eScience* **2** 646–54

[12] Yan D, Zhao S, Zhang Y, Wang H and Zang Z 2022 Highly efficient emission and high-CRI warm white light-emitting diodes from ligand-modified CsPbBr3 quantum dots *Opto-Electronic Advances* **5**

[13] Li X, Cai W, Guan H, Zhao S, Guo S, Cao C, Liu M and Zang Z 2021 Highly stable CsPbBr3 quantum dots by silica-coating and ligand modification for white light-emitting diodes and visible light communication *Chemical Engineering Journal* **419**

[14] Guan H, Zhao S, Wang H, Yan D, Wang M and Zang Z 2020 Room temperature synthesis of stable single silica-coated CsPbBr3 quantum dots combining tunable red emission of Ag–In–Zn–S for High-CRI white light-emitting diodes *Nano Energy* **67**

[15] Kalkal A, Pradhan R, Kadian S, Manik G and Packirisamy G 2020 Biofunctionalized Graphene Quantum Dots Based Fluorescent Biosensor toward Efficient Detection of Small Cell Lung Cancer *ACS Appl Bio Mater* **3**

[16] Kadian S, Manik G, Kalkal A, Singh M and Chauhan R P 2019 Effect of sulfur doping on fluorescence and quantum yield of graphene quantum dots: an experimental and theoretical investigation *Nanotechnology*

[17] Kadian S and Manik G 2020 Sulfur doped graphene quantum dots as a potential sensitive fluorescent probe for the detection of quercetin *Food Chem*

[18] He Y, Zhong Y, Peng F, Wei X, Su Y, Lu Y, Su S, Gu W, Liao L and Lee S T 2011 One-pot microwave synthesis of water-dispersible, ultraphoto- and pH-stable, and highly fluorescent silicon quantum dots *J Am Chem Soc*

[19] Zhong Y, Peng F, Bao F, Wang S, Ji X, Yang L, Su Y, Lee S T and He Y 2013 Large-scale aqueous synthesis of fluorescent and biocompatible silicon nanoparticles and their use as highly photostable biological probes *J Am Chem Soc*

[20] Sun Z, Xie H, Tang S, Yu X F, Guo Z, Shao J, Zhang H, Huang H, Wang H and Chu P K 2015 Ultrasmall Black Phosphorus Quantum Dots: Synthesis and Use as Photothermal Agents *Angewandte Chemie - International Edition*

[21] Zhang X, Xie H, Liu Z, Tan C, Luo Z, Li H, Lin J, Sun L, Chen W, Xu Z, Xie L, Huang W and Zhang H 2015 Black phosphorus quantum dots *Angewandte Chemie - International Edition*

[22] Li S, Chen D, Zheng F, Zhou H, Jiang S and Wu Y 2014 Water-soluble and lowly toxic sulphur quantum dots *Adv Funct Mater*

[23] Kalkal A, Kadian S, Pradhan R, Manik G and Packirisamy G 2021 Recent advances in graphene quantum dot-based optical and electrochemical (bio)analytical sensors *Mater. Adv.* **2** 5513–41

[24] Kadian S, Tailor N K, Chaulagain N, Shankar K, Satapathi S and Manik G 2021 Effect of sulfur-doped graphene quantum dots incorporation on morphological, optical and electron transport properties of CH3NH3PbBr3 perovskite thin films *Journal of Materials Science: Materials in Electronics* **32** 17406–17

[25] Boyd D A 2016 Sulfur and Its Role In Modern Materials Science *Angewandte Chemie - International Edition*

[26] Je S H, Buyukcakir O, Kim D and Coskun A 2016 Direct Utilization of Elemental Sulfur in the Synthesis of Microporous Polymers for Natural Gas Sweetening *Chem*

[27] Tian T, Hu R and Tang B Z 2018 Room Temperature One-Pot Conversion from Elemental Sulfur to Functional Polythioureas through Catalyst-Free Multicomponent Polymerizations *J Am Chem Soc*

[28] Shen L, Wang H, Liu S, Bai Z, Zhang S, Zhang X and Zhang C 2018 Assembling of Sulfur Quantum Dots in Fission of Sublimed Sulfur *J Am Chem Soc*

[29] Wang H, Wang Z, Xiong Y, Kershaw S V, Li T, Wang Y, Zhai Y and Rogach A L 2019 Hydrogen Peroxide Assisted Synthesis of Highly Luminescent Sulfur Quantum Dots *Angewandte Chemie - International Edition*

[30] Xiao L, Du Q, Huang Y, Wang L, Cheng S, Wang Z, Wong T N, Yeow E K L and Sun H 2019 Rapid Synthesis of Sulfur Nanodots by One-Step Hydrothermal Reaction for Luminescence-Based Applications *ACS Appl Nano Mater*

[31] Song Y, Tan J, Wang G, Gao P, Lei J and Zhou L 2020 Oxygen accelerated scalable synthesis of highly fluorescent sulfur quantum dots *Chem Sci*

[32] Chen B, Li F, Li S, Weng W, Guo H, Guo T, Zhang X, Chen Y, Huang T, Hong X, You S, Lin Y, Zeng K and Chen S 2013 Large scale synthesis of photoluminescent carbon nanodots and their application for bioimaging *Nanoscale*

[33] Bang J H and Suslick K S 2010 Applications of ultrasound to the synthesis of nanostructured materials *Advanced Materials*

[34] Cai J, Miao Y Q, Lin B Z, Ma P, Li L and Fan H M 2017 Large-Scale, Facile Transfer of Oleic Acid-Stabilized Iron Oxide Nanoparticles to the Aqueous Phase for Biological Applications *Langmuir* **33**

[35] Soutelo-María A, Dubois J L, Couturier J L and Cravotto G 2018 Oxidative cleavage of fatty acid derivatives for monomer synthesis *Catalysts* **8**

[36] Manan N S A, Aldous L, Alias Y, Murray P, Yellowlees L J, Lagunas M C and Hardacre C 2011 Electrochemistry of sulfur and polysulfides in ionic liquids *Journal of Physical Chemistry B*

[37] Xie X Y, Li L Y, Zheng P S, Zheng W J, Bai Y, Cheng T F and Liu J 2012 Facile synthesis, spectral properties and formation mechanism of sulfur nanorods in PEG-200 *Mater Res Bull* **47**

[38] Lu H, Zhang H, Li Y and Gan F 2021 Sensitive and selective determination of tetracycline in milk based on sulfur quantum dot probes *RSC Adv* **11**

[39] Ahn C.C. and Krivanek O.L EELS Atlas: A Reference Guide of Electron Energy Loss Spectra Covering All Stable Elements

[40] Padalkar S, Hulleman J D, Kim S M, Rochet J C, Stach E A and Stanciu L A 2008 Protein-templated semiconductor nanoparticle chains *Nanotechnology* **19**

[41] Song Y, Tan J, Wang G, Gao P, Lei J and Zhou L 2020 Oxygen accelerated scalable synthesis of highly fluorescent sulfur quantum dots *Chem Sci* **11**

[42] Anon *Sulfur R040135 - RRUFF Database: Raman, X-ray, Infrared, and Chemistry*

[43] Kooter I M, Pierik A J, Merkx M, Averill B A, Moguilevsky N, Bollen A and Wever R 1997 Difference fourier transform infrared evidence for ester bonds linking the heine group in myeloperoxidase, lactoperoxidase, and eosinophil peroxidase [5] *J Am Chem Soc*

[44] Ibarra J, Melendres J, Almada M, Burboa M G, Taboada P, Juárez J and Valdez M A 2015 Synthesis and characterization of magnetite/PLGA/chitosan nanoparticles *Mater Res Express*

[45] Zhang L, He R and Gu H C 2006 Oleic acid coating on the monodisperse magnetite nanoparticles *Appl Surf Sci*

[46] Kadian S, Manik G, Das N and Roy P 2020 Targeted bioimaging and sensing of folate receptor-positive cancer cells using folic acid-conjugated sulfur-doped graphene quantum dots *Microchimica Acta*

[47] Kadian S, Manik G, Das N, Nehra P, Chauhan R P and Roy P 2020 Synthesis, characterization and investigation of synergistic antibacterial activity and cell viability of silver and sulfur doped graphene quantum dot (Ag@S-GQDs) nanocomposites *J Mater Chem B*

[48] Wang H, Wang Z, Xiong Y, Kershaw S V, Li T, Wang Y, Zhai Y and Rogach A L 2019 Hydrogen Peroxide Assisted Synthesis of Highly Luminescent Sulfur Quantum Dots *Angewandte Chemie - International Edition* **58**

[49] Qiu L, Zou K and Xu G 2013 Investigation on the sulfur state and phase transformation of spent and regenerated S zorb sorbents using XPS and XRD *Appl Surf Sci* **266**

[50] Arshad F and Sk M P 2020 Luminescent Sulfur Quantum Dots for Colorimetric Discrimination of Multiple Metal Ions *ACS Appl Nano Mater*

[51] Zhang C, Zhang P, Ji X, Wang H, Kuang H, Cao W, Pan M, Shi Y E and Wang Z 2019 Ultrasonication-promoted synthesis of luminescent sulfur nano-dots for cellular imaging applications *Chemical Communications*

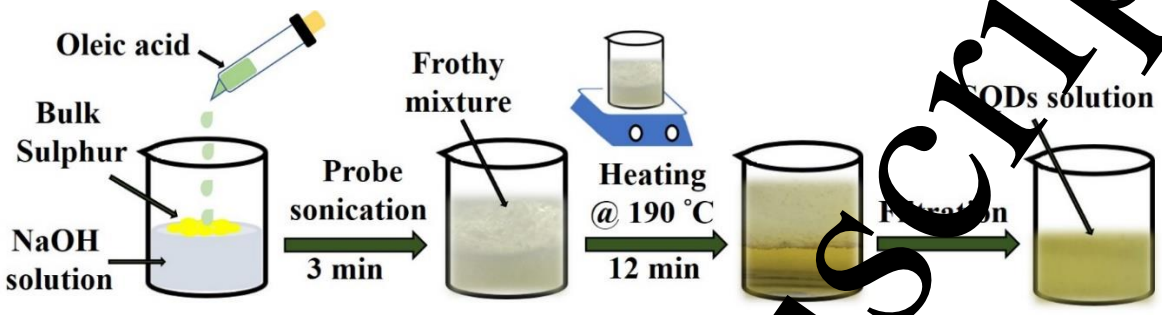

Scheme 1. Schematic illustration of the synthesis process of SQDs.

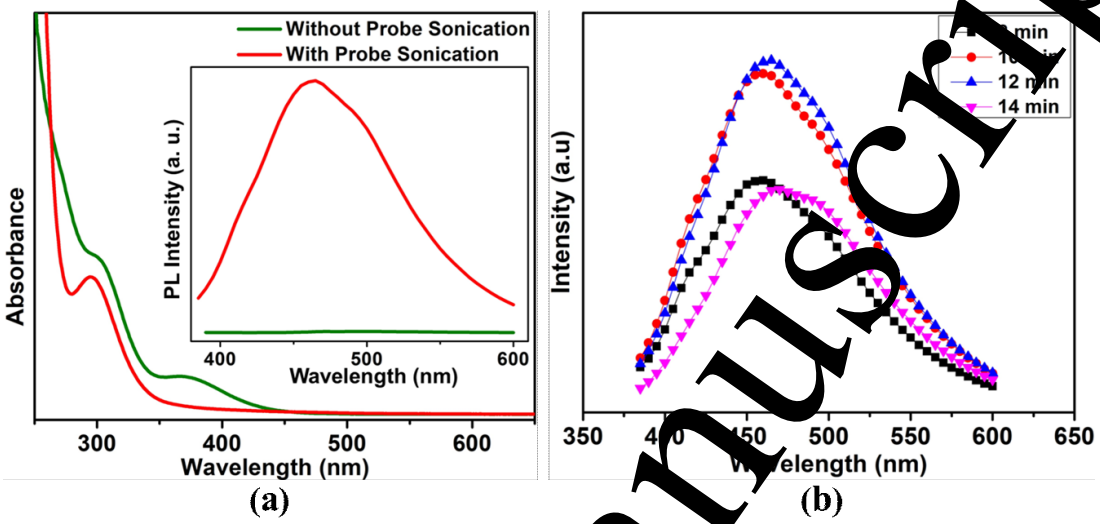

Fig. 1. (a) UV-Vis absorption and PL spectra (inset) of SQDs with and without probe sonication assistance and (b) PL spectra of SQDs samples obtained at different heating time durations (8, 10, 12 and 14 min).

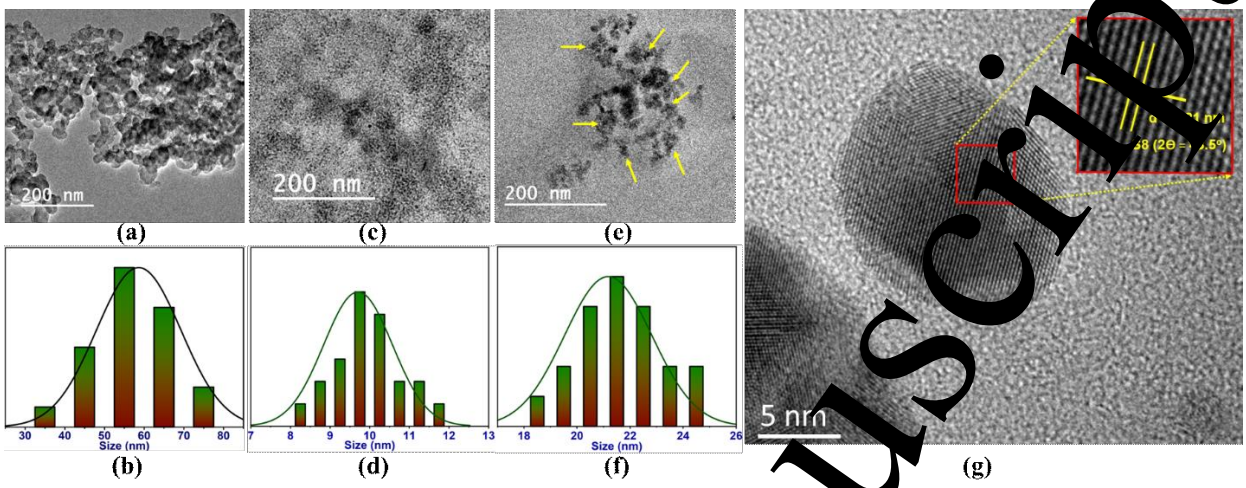

Fig. 2. TEM image and size distribution histogram of (a and b) non-fluorescent S-dots obtained after 14 min heat *without* any probe sonication treatment, (c and d) SQDs prepared *with* probe sonication followed by 12 min and (e and f) 14 min heat; (g) HR-TEM image of SQDs prepared *with* probe sonication followed by 12 min heat.

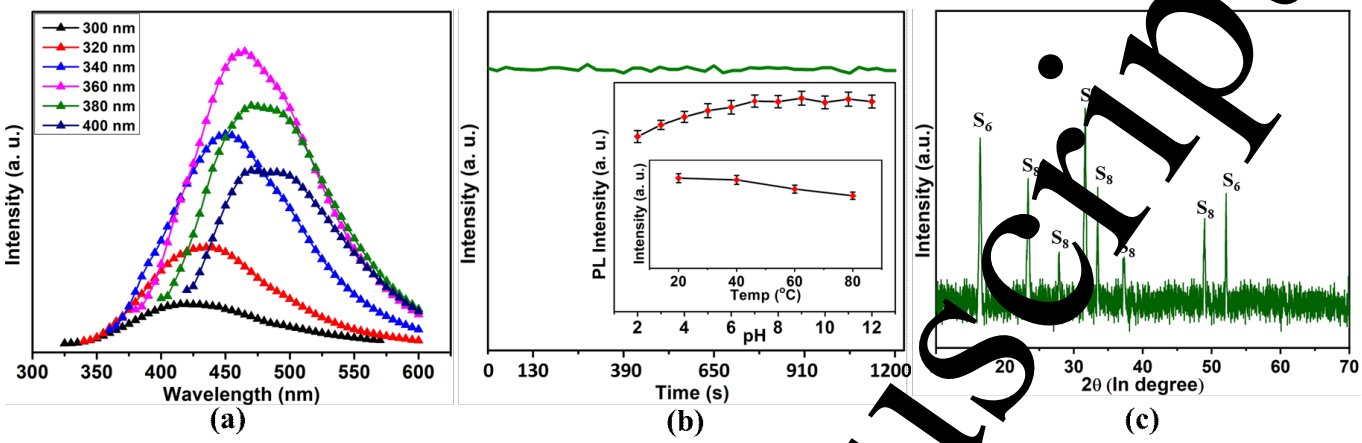

Fig. 3. (a) PL emission spectra of SQDs at different excitation wavelengths ranging from 300 nm to 400 nm, (b) effects of continuous UV irradiation for 20 min, different pH (2–12) and temperature (20-80°C) environments (inset) on the fluorescence intensity of SQDs, and (c) XRD patterns of as-prepared SQDs.

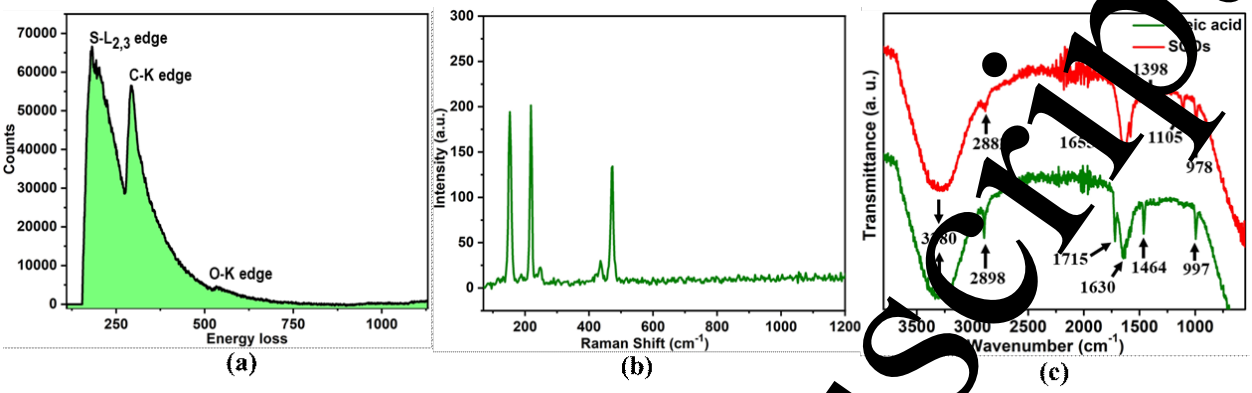

Fig. 4. Illustration of (a) EELS of as-prepared SQDs, (b) Raman spectra of as-prepared SQDs, and (c) FTIR spectra of oleic acid (green curve) and as-prepared SQDs (red curve).

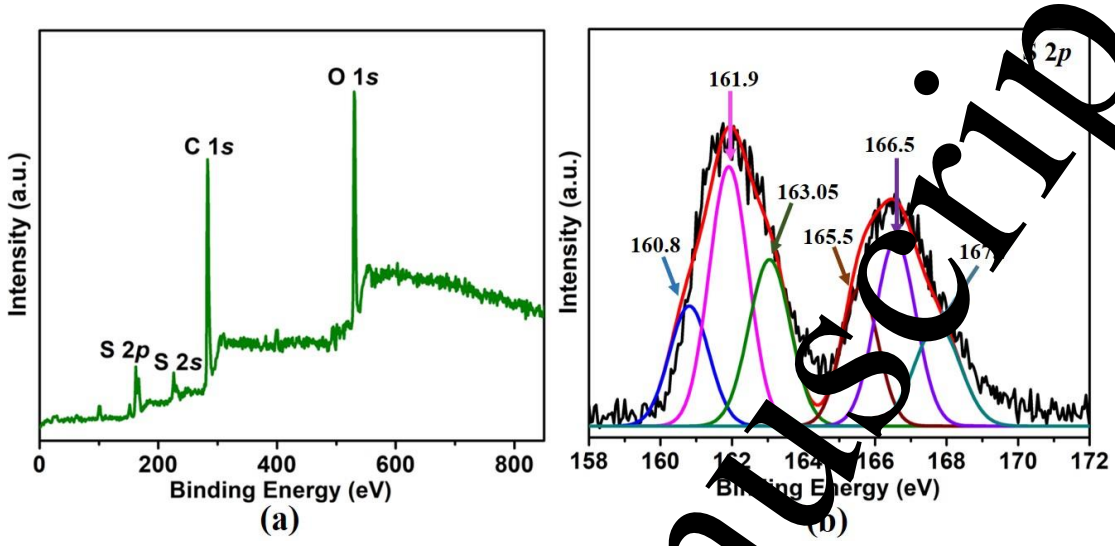

Fig. 5. (a) XPS spectrum and (b) high-resolution deconvoluted *S 2p* spectrum of as-prepared SQDs.

Table 1. Comparison of our proposed strategy and previously reported approaches for the synthesis of SQDs

Strategy	**Precursors**	**Passivating agent**	**Reaction time**	**QY (%)**	**Ref**
Phase interfacial	CdSQDs & HNO_3	--	36 h	0.549	[22]
Assemble-fission	Bulk S & NaOH	PEG	125 h	3.8	[28]
H_2O_2 assisted	Bulk S & NaOH	PEG	125 h	23	[29]
Ultrasonication	Bulk S & Na_2S	PEG	12 h	2.1	[51]
Oxygen accelerated	Bulk S & NaOH	PEG	10 h	1.08	[31]
Hydrothermal	Bulk S & NaOH	PEG	4 h	4.02	[30]
Probe sonication	**Bulk S & NaOH**	**Oleic acid**	**15 min**	**10.4**	**This work**